

Long non-coding RNA LINC00672 contributes to p53 protein-mediated gene suppression and promotes endometrial cancer chemosensitivity

Received for publication, September 15, 2016, and in revised form, February 19, 2017. Published, JBC Papers in Press, February 23, 2017, DOI 10.1074/jbc.M116.758508

Wei Li^{‡1}, Hua Li^{§1}, Liyuan Zhang[¶], Min Hu^{||}, Fang Li[‡], Jieqiong Deng[‡], Mingxing An[‡], Siqi Wu[‡], Rui Ma[‡], Jiachun Lu^{**}, and Yifeng Zhou^{‡2}

From the [‡]Department of Genetics, Medical College of Soochow University, Suzhou 215123, the [§]Department of Obstetrics and Gynecology, Third Hospital, Peking University, Beijing 100191, the Departments of [¶]Radiotherapy and Oncology and ^{||}Obstetrics and Gynecology, The Second Affiliated Hospital of Soochow University, San Xiang Road No. 1055, Suzhou 215004, and the ^{**}Institute for Chemical Carcinogenesis, The State Key Lab of Respiratory Disease, Guangzhou Medical University, Guangzhou 510182, China

Edited by Eric R. Fearon

Thousands of long intergenic non-protein coding RNAs (lincRNAs) have been identified in mammals in genome-wide sequencing studies. Some of these RNAs have been consistently conserved during the evolution of species and could presumably function in important biologic processes. Therefore, we measured the levels of 26 highly conserved lincRNAs in a total of 176 pairs of endometrial carcinoma (EC) and surrounding non-tumor tissues of two distinct Chinese populations. Here, we report that a lincRNA, *LINC00672*, which possesses an ultra-conserved region, is aberrantly down-regulated during the development of EC. Nevertheless, *LINC00672* is a p53-targeting lincRNA acting along with heterogeneous nuclear ribonucleoproteins as a suppressive cofactor, which locally reinforces p53-mediated suppression of *LASP1*, an evolutionarily conserved neighboring gene of *LINC00672* and putatively associated with increased tumor aggressiveness, during anti-tumor processes. *LINC00672* overexpression could lower the levels of *LASP1* and slow the development of malignant phenotypes of EC both *in vitro* and *in vivo*. Moreover, *LINC00672* significantly increased the 50% inhibitory concentration of paclitaxel in EC cells and increased the sensitivity of xenograft mice to paclitaxel. These findings indicate that *LINC00672* can influence *LASP1* expression as a locus-restricted cofactor for p53-mediated gene suppression, thus impacting EC malignancies and chemosensitivity to paclitaxel.

Endometrial carcinoma (EC),³ one of the most common gynecologic malignancies, has significantly increased in both

This work was supported by National Scientific Foundation of China Grant 81472630, by Priority Academic Program Development of Jiangsu Higher Education Institutions, Jiangsu Provincial Special Program of Clinical Medical Science Grant BL2014040, Science Foundation for Distinguished Young Scholars in Jiangsu Grant BK20160008, National Key R&D Program of China Grant 2016YFC1302100, and Suzhou Science and Technology Development Program Grant SZS201509. The authors declare that they have no conflicts of interest with the contents of this article.

This article contains supplemental Tables S1–S3 and Figs. S1 and S2.

¹ Both authors contributed equally to this work.

² To whom correspondence should be addressed: Medical College of Soochow University, Suzhou 215123, China. Tel.: 86-512-65884720; Fax: 86-512-65884720; E-mail: zhoyifeng@suda.edu.cn.

³ The abbreviations used are: EC, endometrial carcinoma; lincRNA, long intergenic ncRNA; hnRNP, heterogeneous nuclear ribonucleoprotein; qRT,

incidence and mortality over the past decade (1). The development of new treatment modalities, diagnostic technologies, and prevention approaches for this disease requires a better understanding of the molecular mechanisms that underlie endometrial carcinogenesis. Although previous studies have documented alterations in many oncogenes and tumor suppressor genes involved in EC, the molecular and genetic basis of endometrial carcinogenesis remains largely unknown (2).

The human transcriptome contains both a large number of protein-coding messenger RNAs (mRNAs) and a large set of non-protein-coding transcripts whose functions are structural, regulatory, or unknown. Among the various types of non-coding RNAs (ncRNAs), long intergenic ncRNAs (lincRNAs) have been described as RNA molecules longer than 200 nucleotides. lincRNAs are also capped, polyadenylated, and often spliced. However, they do not overlap with protein-coding genes or with previously documented classes of ncRNAs (3, 4). A growing body of evidence shows that lincRNAs participate in a wide range of cellular biologic processes, including the regulation of epigenetic signatures and gene expression, the maintenance of pluripotency, and the differentiation of embryonic stem cells (5–8). Because lincRNAs exhibit tissue- and development-specific expression patterns, some studies have implicated lincRNAs in a variety of disease states, including human cancer (9, 10). Moreover, altered lincRNA levels can result in an aberrant expression of gene products that may contribute to cancer (5, 11, 12).

Over the past several decades, thousands of lincRNAs have been identified in humans and mice, of which only a few have orthologs outside of these two species (4, 13). However, Ulitsky *et al.* (14) have identified over 550 distinct lincRNAs in zebrafish, among which 26 lincRNAs exhibit both a detectable sequence similar to putative human orthologs and conserved genomic sites throughout vertebrate evolution. High sequence conservation suggests that these lincRNAs may possess conserved structural features, which have conferred crucial func-

quantitative RT; RNAP, RNA polymerase; nt, nucleotide; LNA, locked nucleic acid; RACE, rapid amplification of cDNA end; RIP, RNA immunoprecipitation; PI, propidium iodide.

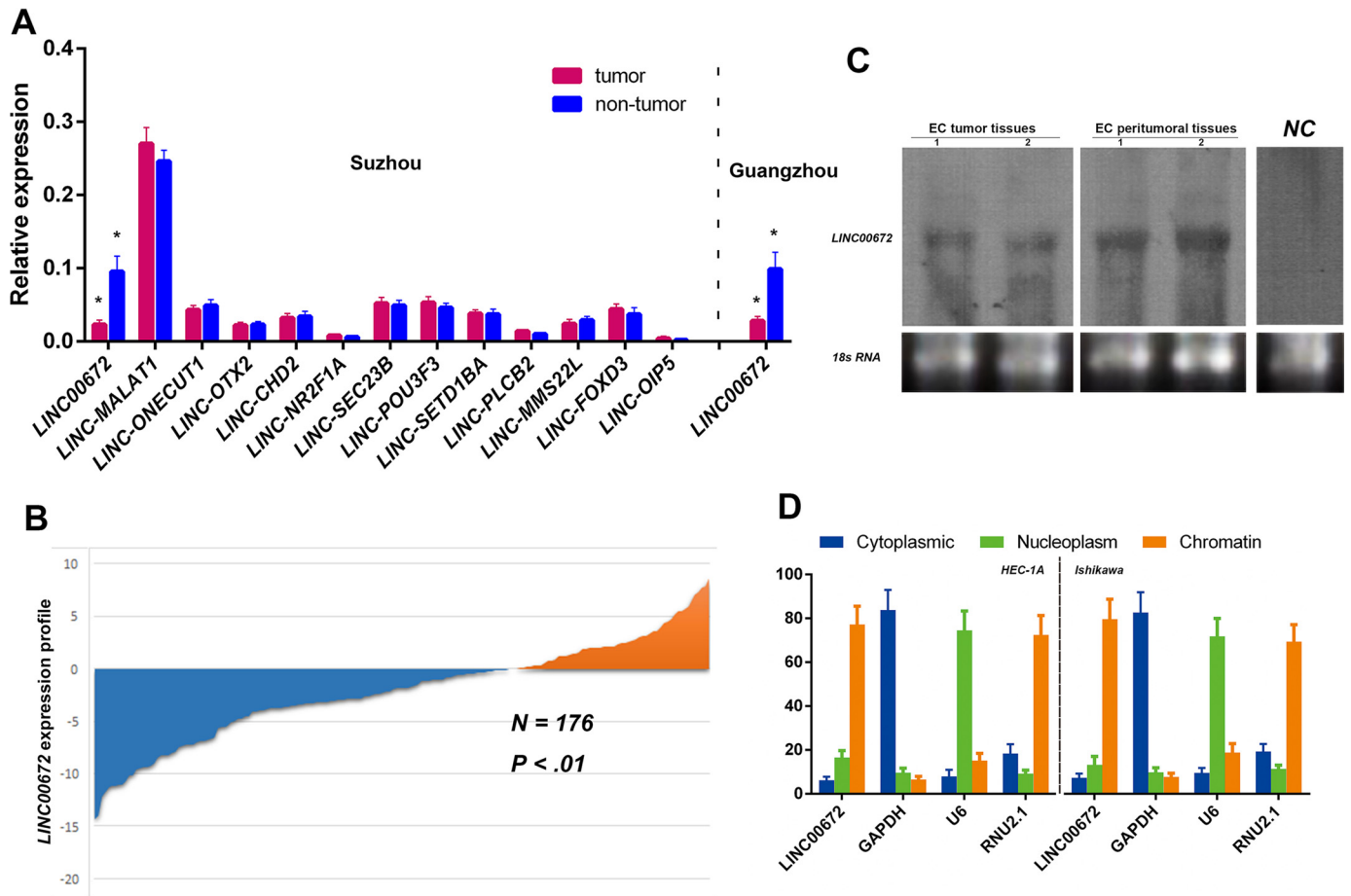


Figure 1. LincRNA expression patterns in EC samples and cells. *A*, expression of 13 candidate lincRNAs in EC and matched non-tumor endometrial specimens from 104 patients in the Suzhou cohort; *LINC00672* were also determined in 72 patients in the Guangzhou cohort. * indicates *p* values calculated by paired Student's *t* test were below 0.05. *B*, *LINC00672* expressed at lower level in ~68.8% (121/176) of all EC patients, compared with matched non-cancerous samples. The expression level was analyzed by qRT-PCR and normalized to *GAPDH*. Data are represented as mean ± S.E. from three independent experiments. *N*, non-neoplastic tissues; *T*, tumor tissues. *C*, Northern blotting of *LINC00672* in two pairs of EC tissue samples (randomly selected). *NC*, negative control. *D*, relative abundance of *LINC00672* transcript in cytoplasm, nucleus, and chromatin in EC cells. *GAPDH*, *U6*, and *RNU2.1* were used, respectively, as cytoplasmic, nuclear, and chromatin-associated controls (average three experiments ± S.E.).

tions upon them throughout evolution. Furthermore, recent studies have demonstrated that lincRNAs could regulate the expression of neighboring protein-coding genes by functioning as enhancers or epigenetic regulatory elements (7, 15). The relative location of the conserved sequences has led us to believe that these lincRNAs may function predominantly in association with their conserved neighboring protein-coding genes. Although the importance of lincRNAs in normal physiologic processes and disease is increasingly recognized, our knowledge of cancer-related lincRNA, however, remains limited. Therefore, it is particularly important to elucidate the function of these highly conserved lincRNAs and their working mechanism in EC.

Here, we report the identification of *LINC00672* with highly conserved sequence and genome location, which is significantly down-regulated during the progression of the FIGO stages of EC. In addition, *LINC00672* also influences the chemotherapeutic effects of paclitaxel. Biochemical assays have demonstrated that *LINC00672* acts as a p53-mediated suppressive cofactor that locally reinforces *LASPI* repression during anti-tumor processes. Moreover, *LINC00672* expression may impact the IC₅₀ value of paclitaxel and the chemosensitivity of

EC cells *in vitro* and *in vivo*, suggesting a potential clinical value for chemotherapy of EC patients.

Results

lincRNA expression patterns in EC samples

After the categorization and selection described under "Experimental procedures," we first performed qRT-PCR analysis to identify the expression patterns of the selected 13 candidate lincRNAs in 104 pairs of EC tissue samples from an Eastern Chinese population (Suzhou center). The results showed that the expression levels of *LINC00672* were significantly higher (~4.15-fold, *p* < 0.001) in adjacent non-neoplastic tissues than in tumor tissues. No other lincRNAs showed significant difference in expression level between EC and adjacent normal tissues (Fig. 1A).

The results were also confirmed in 72 other pairs of EC and adjacent non-neoplastic tissues of a population in southern China (Guangzhou center). The *LINC00672* levels were notably higher (~3.5-fold, *p* < 0.001) in adjacent non-neoplastic tissues than in tumor tissues (Fig. 1A). A pooled analysis of both the discovery and validation datasets demonstrated that the

LINC00672 expression was at a lower level among 68.8% (121/176) of all the EC patients (Fig. 1B).

Biologic characterization of *LINC00672*

As discovered by Ulitsky *et al.* (14), the sequence of *LINC00672* is detectable and similar to the putative mammalian orthologs that are restricted to a single short region of high conservation, and its genomic location is also conserved (it conservatively neighbors the *LASPI* gene in the same orientation throughout species evolution). We then detected *LINC00672* in the total RNA of two pairs of human EC tissue samples using Northern blotting (Fig. 1C). To determine the cellular localization of *LINC00672*, we fractionated EC cell lines into nuclear and cytoplasmic fractions and thoroughly separated the chromatin of the cells from the nuclear fraction. The data revealed that *LINC00672* was strongly enriched in the chromatin fraction of both HEC-1A and Ishikawa cells (Fig. 1D).

To further verify the coding potential of *LINC00672*, we re-analyzed a dataset of human lymphoblastoid cell ribosome sequencing profiling and measured the ribosome occupancy level at the *LASPI* gene locus (16, 17). As expected, the ribosome profiling reads are highly concentrated within the coding region of the *LASPI* gene but not *LINC00672* (Fig. 2A).

LINC00672 is a direct transcriptional target of p53

A previous genome-wide analysis of the human p53 transcriptional network (18) indicated that *LINC00672* might be a p53 transcriptional target. To confirm this possibility, we examined the enrichment of evolutionarily conserved p53-binding motifs in the promoter of *LINC00672* and found that the promoter region of *LINC00672* contained highly conserved canonical p53-binding motifs. Next, we cloned the proximal promoter region of *LINC00672* to construct reporter plasmids (pGL3-*LINC00672*) and performed luciferase assays in normal EC cells and cells with p53 pharmacologically inhibited (supplemental Fig. 2, A and B). As illustrated in Fig. 2B, luciferase activity significantly decreased in the p53-inhibited cells, compared with the control cells. We performed chromatin immunoprecipitation (ChIP) experiments to determine whether p53 directly binds to the sites containing the consensus motifs *in vivo*. The results showed significant increases in p53, RNAP II, and P300 enrichment at the site within the promoter of *LINC00672*. No enrichment was shown at the negative control sites that contain irrelevant regions (Fig. 2C). Finally, we examined *LINC00672* expression in the tissues from p53^{-/-} and WT mice. The results also revealed that the absence of p53 influences the expression of *LINC00672* in uterus (Fig. 2D). The PhyloP algorithm from UCSC discovered a region of 125 nt from human *LINC00672* with deep evolutionary conservation across 100 vertebrates (Fig. 2E), prompting a crucial role of this region. We then used 5'- and 3'-rapid amplification of cDNA ends (RACE) to determine the transcriptional initiation and termination sites of *LINC00672* (supplemental Fig. 1, A–C). We analyzed the RNA folding potential of the full-length *LINC00672* and the 125-nt truncated version of *LINC00672* based on the conserved sequence and the compensatory changes in base-wise conservation. The predicted folding

structure of *LINC00672* greatly changed with the deep conserved 125-nt region removed (supplemental Fig. 1D).

LINC00672 regulates the cell cycle in EC cells

We further investigated the effects of *LINC00672* on the cell cycle by analyzing PI-stained EC cells with fluorescence-activated cell sorting (FACS). The representative results of the cell cycle distribution in the empty vector, *LINC00672*, and *LINC00672*-mutant lentiviruses transfected EC cells (supplemental Fig. 2C), and the locked nucleic acid (LNA) Gapmers (LNA-based antisense oligonucleotides strategy) targeting *LINC00672*-treated EC cells are shown in Fig. 3, A and B. Flow cytometric analysis indicated that *LINC00672* overexpression resulted in a significant accumulation of HEC-1A and Ishikawa cells in G₂-M phase, whereas there were no significant changes in the number of cells transfected with the truncated version of *LINC00672* (removed the 125-nt conserved region) (Fig. 3A). In contrast, the treatment of LNAs targeting *LINC00672* resulted in a significant decrease in cell number in the G₂-M phase (Fig. 3B). Also, we investigated the effects of *LINC00672* on EC cell apoptosis, and no significant changes of cell apoptosis were detected (supplemental Fig. 2, D and E).

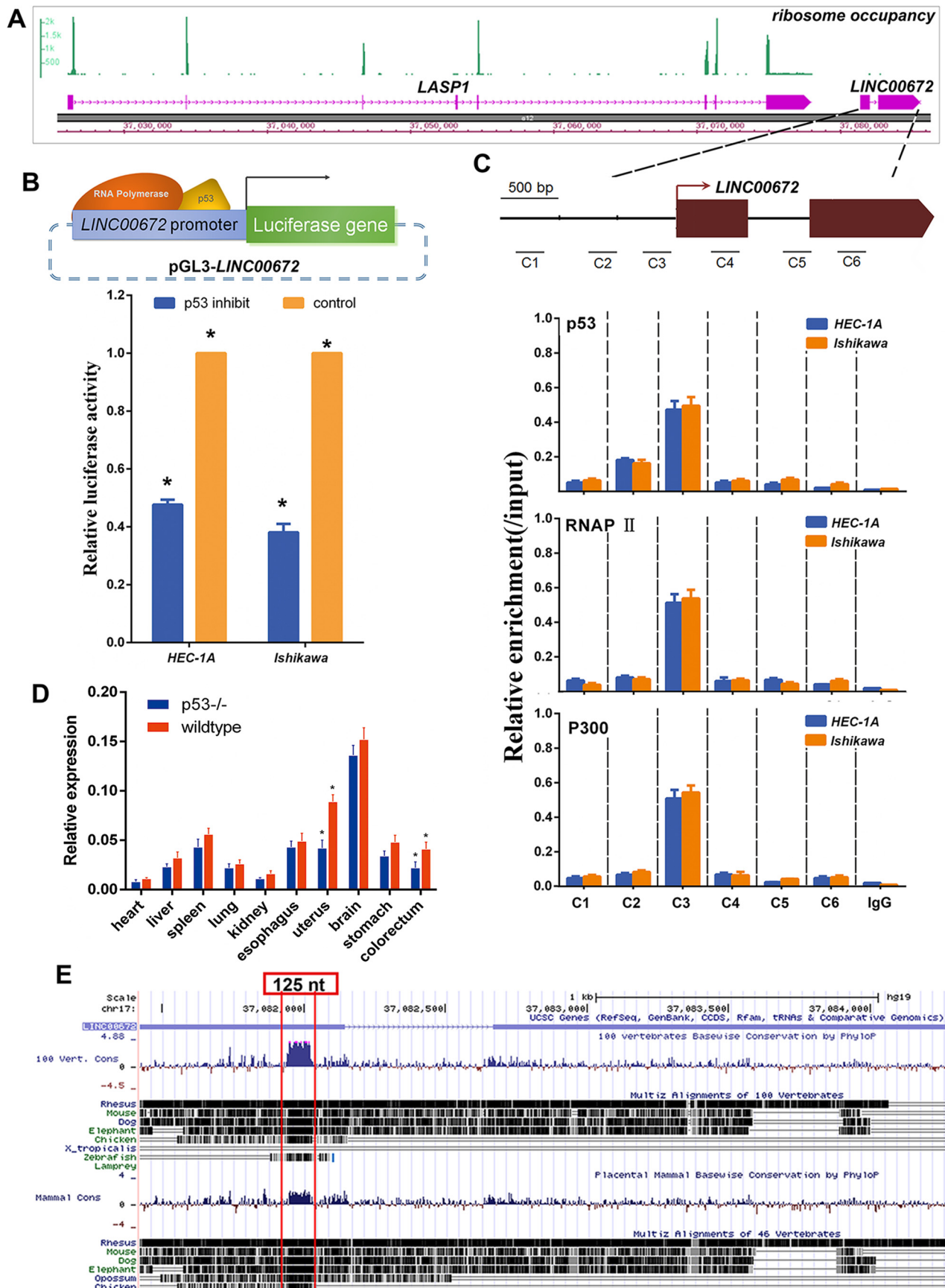
Effects of ectopic *LINC00672* expression on EC cell proliferation and migration

We next examined the effects of *LINC00672* on cell proliferation and found that the overexpression of *LINC00672* in endometrial cancer cells HEC-1A and Ishikawa substantially reduced cell proliferation. Transfection with the mutant version of *LINC00672* makes no significant changes in the control cells (Fig. 3C), but knockdown of *LINC00672* by LNA Gapmers significantly increased EC cell proliferation (Fig. 3D). We also performed a colony formation assay using HEC-1A and Ishikawa cells and found that the overexpression of *LINC00672* markedly decreased the colony formation ability of endometrial cancer cells. The LNA-mediated knockdown of *LINC00672* conspicuously increased EC cells colony formation ability, whereas the impact of truncated *LINC00672* transfection on EC cell viability is not significant (Fig. 3, E and F).

To investigate the influence of *LINC00672* expression on the migration ability of EC cells, we conducted transwell and wound-healing assays, using EC cells with *LINC00672* overexpressed and knocked down. As illustrated in Fig. 4, A–D, both the transwell and wound-healing assays demonstrated that the migration capability of HEC-1A and Ishikawa cells was significantly suppressed by *LINC00672* overexpression and both assays were stimulated by *LINC00672* knockdown. But the mutant version of *LINC00672* had no significant impact on the migration and invasion of EC cells.

Effects of *LINC00672* levels on EC tumor growth

To probe the effects of *LINC00672* on cancer cell dynamics *in vivo*, we injected *LINC00672*-knockdown cells, *LINC00672* up-regulated cells, *LINC00672*-mutant cells and control cells into the hind flanks of nude mice. We observed that the growth of *LINC00672* up-regulated xenografts was significantly inhibited, compared with that of control xenografts. But xenografts of the mutant version of *LINC00672* showed no significant dif-



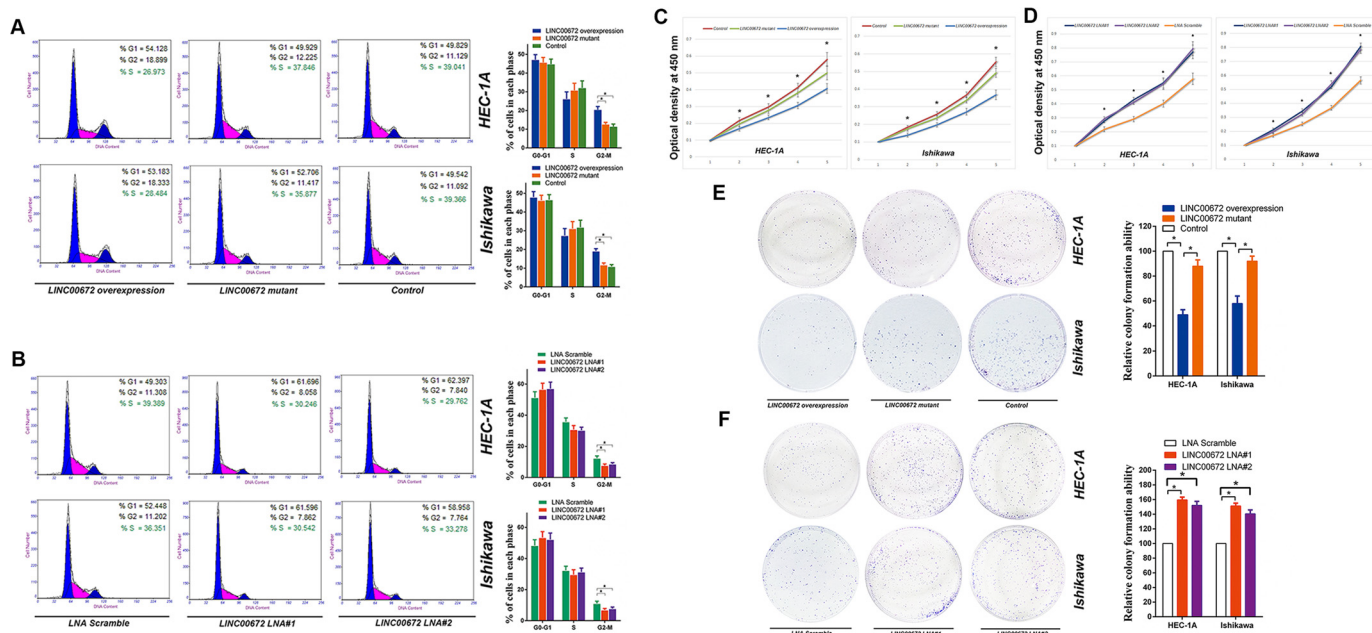


Figure 3. Effects of ectopic *LINC00672* expression on EC cells. *A*, cell cycle analysis of HEC-1A and Ishikawa cells after transfection with *LINC00672*, *LINC00672*-mutant, and control lentiviruses. Results are represented as mean \pm S.D. based on three independent experiments (*, $p < 0.05$). *B*, cell cycle analysis of HEC-1A and Ishikawa cells after transfection with *LINC00672* LNA#1, *LINC00672* LNA#2, and LNA scramble. Results are represented as mean \pm S.D. based on three independent experiments (*, $p < 0.05$). *C*, HEC-1A and Ishikawa cells were seeded in 96-well plates after transfection with *LINC00672*-mutant, and control lentiviruses. Cell proliferation was assessed daily for 4 days using the Cell Counting Kit-8; data are represented as mean \pm S.D. ($n = 6$, *, $p < 0.05$). *D*, HEC-1A and Ishikawa cells were seeded in 96-well plates after transfection with *LINC00672* LNA#1, *LINC00672* LNA#2, and LNA scramble. Cell proliferation was assessed daily for 4 days using the Cell Counting Kit-8; data are represented as mean \pm S.D. ($n = 6$, *, $p < 0.05$). *E*, representative colony formation assay in HEC-1A and Ishikawa cells after transfection with *LINC00672*, *LINC00672*-mutant, and control lentiviruses. *Right panel* is the quantitative analysis of colony formation. Colony numbers of control cells were set to 100%. Values are expressed as mean \pm S.D. from three experiments (*, $p < 0.05$). *F*, representative colony formation assay in HEC-1A and Ishikawa cells after transfection with *LINC00672* LNA#1, *LINC00672* LNA#2, and LNA scramble. Colony numbers of scramble LNA cells were set to 100%. Values are expressed as mean \pm S.D. from three experiments (*, $p < 0.05$).

ference in the control cells (Fig. 4E). The growth of *LINC00672*-knockdown xenografts was substantially promoted, compared with that of control xenografts (Fig. 4F and supplemental Fig. 2, F and G).

LINC00672 interacts with hnRNP F/H to repress *LASP1* transcription

To determine whether the expression pattern of *LINC00672* correlated with the expression of *LASP1*, we detected a negative correlation between the expression levels of *LINC00672* and *LASP1* in 62 pairs of randomly selected EC tissues (Fig. 5A). To further evaluate the effects of *LINC00672* on *LASP1* gene expression, we analyzed the expression of *LASP1* gene. We found that the expression diminished when *LINC00672* was overexpressed. However, it was up-regulated when *LINC00672* was knocked down in the EC cells (Fig. 5, B and C). Moreover, there were no significant changes in *LASP1* expression in the EC cells transfected with *LINC00672*-mutant lentivirus. The protein level of *LASP1* detected by Western blotting and immunofluorescence assay revealed the same trends in the *LINC00672*-manipulated EC cells (Fig. 5, D–F). We also mea-

sured the expression patterns of three other putative p53 target genes (*p21*, *bax*, and *gadd45*) in *LINC00672*-manipulated EC cells. The results showed no significant impact of *LINC00672* on these genes (supplemental Fig. 2H).

Many lincRNAs have been reported to regulate gene expression via their interaction with several chromatin-regulatory complexes (4, 5, 19), suggesting that lincRNAs can play a general role in the recruitment of transcriptional cofactors to their target genes. To address the hypothesis that *LINC00672* might interact with certain cellular proteins to exert its anti-tumor effects, we first used catRAPID software (20) to predict the proteins that might interact with *LINC00672*. Interestingly, the binding predictions showed that heterogeneous nuclear ribonucleoprotein F and H (hnRNP F and hnRNP H) bind precisely to the ~ 125 -nt highly evolutionarily conserved sequence in the 5'-portion of *LINC00672*, and this interaction was specifically identified as NPInter (ncRNA-protein interactions) according to the catRAPID discriminative analysis. To verify this prediction, we performed an RNA-pulldown experiment followed by Western blotting against hnRNP F and hnRNP H. A strong signal for hnRNP F was detected in proteins that were pulled

Figure 2. Biologic characterization of *LINC00672*. *A*, ribosome occupancy at the *LASP1* and *LINC00672* locus. The green peaks indicate reads density that mapped at the region. *B*, luciferase reporter assay in HEC-1A and Ishikawa cells after pharmacologically p53 inhibition and the reporter constructs expressing the luciferase gene under *LINC00672* promoter segment. Data are presented as the mean \pm S.E. of quadruplicate assays. *C*, chromatin immunoprecipitation showing p53, RNAP II, and p300 occupancy at the *LINC00672* locus in HEC-1A and Ishikawa cells. Locations of amplicons (C1–C6) are indicated in the above scheme. Values represent the enrichment of bound protein fractions relative to input. Data are represented as mean \pm S.D. of three independent experiments ($n = 3$). *D*, *LINC00672* expression levels in main organs of p53^{-/-} mice. Data are represented as mean \pm S.D. of four independent experiments ($n = 4$, *, $p < 0.05$). *E*, 100 vertebrates and placental mammal basewise conservation at *LINC00672* locus (obtained from UCSC PhyloP program). The remarkable peak indicates an about 125-nt ultra-conserved region.

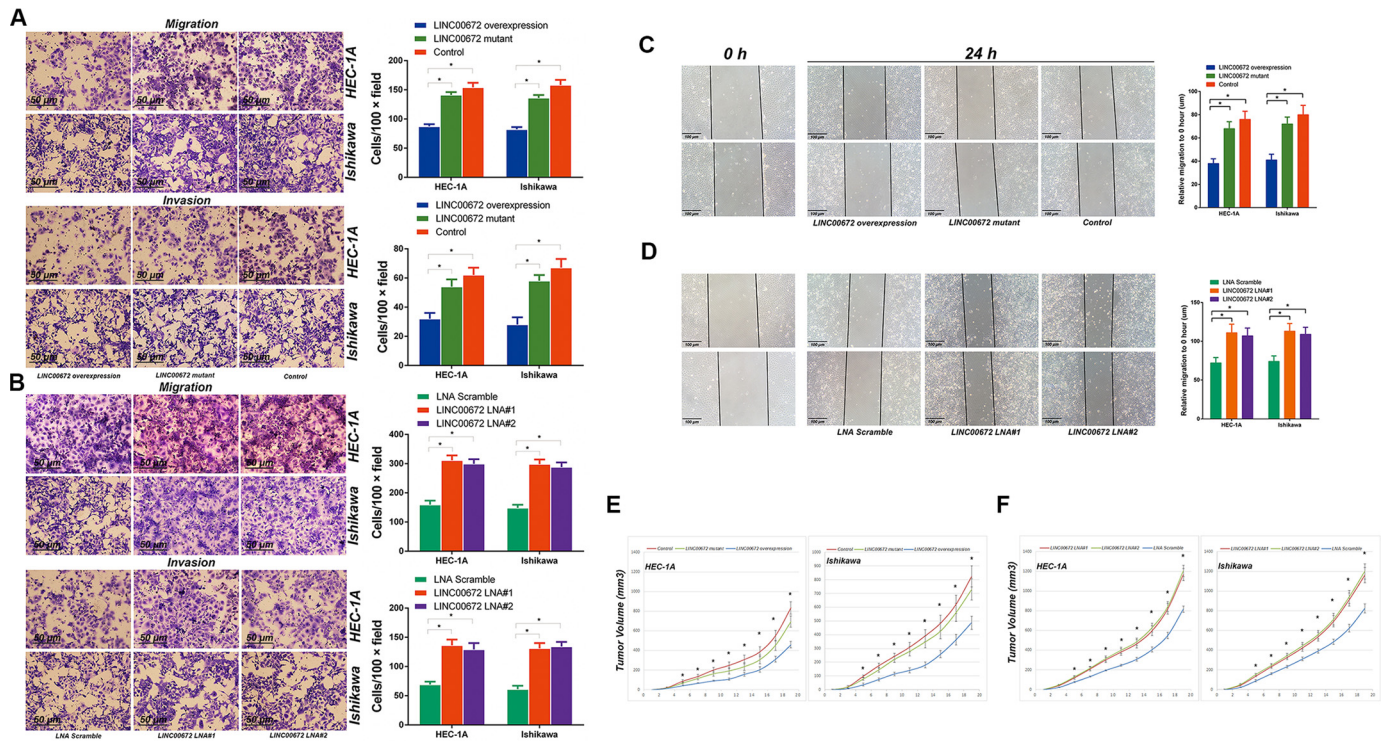


Figure 4. Effects of ectopic LINC00672 expression on EC cells. *A*, migration and invasion of EC cells transfected with *LINC00672*, *LINC00672*-mutant, and control lentiviruses. *Right panel* is the quantification of EC cells that migrated through the membrane without the Matrigel (*upper*) and invaded through Matrigel-coated membrane (*lower*). Asterisk indicates a significant change ($p < 0.05$). *B*, migration and invasion of EC cells transfected with *LINC00672* LNA#1, *LINC00672* LNA#2, and LNA scramble. *Right panel* is the quantification of EC cells that migrated through the membrane without the Matrigel (*upper*) and invaded through Matrigel-coated membrane (*lower*). Asterisk indicates a significant change ($n = 3, p < 0.05$). *C*, wound-healing assay using HEC-1A and Ishikawa cells after transfection with *LINC00672*, *LINC00672*-mutant, and control lentiviruses. *Right panel* is the quantification of the relative migration distance. Asterisk indicates a significant change ($n = 3, p < 0.05$). *D*, wound-healing assay using HEC-1A and Ishikawa cells after transfection with *LINC00672* LNA#1, *LINC00672* LNA#2, and LNA scramble. *Right panel* is the quantification of the relative migration distance. Asterisk indicates a significant change ($n = 3, p < 0.05$). *E*, xenograft mice subcutaneously implanted *LINC00672*-up-regulated, *LINC00672*-mutant, and respective control EC cells were established. *Bars* show S.D. The mean tumor volume from six nude mice of each group are shown (*, $p < 0.05$). *F*, xenograft mice subcutaneously implanted *LINC00672* LNA#1, *LINC00672* LNA#2, and LNA scramble EC cells were established. *Bars* show S.D. The mean tumor volume from six nude mice of each group are shown (*, $p < 0.05$).

down with the sense strand of *LINC00672*, as well as hnRNP H, but not hnRNP D and hnRNP I (Fig. 5G). Furthermore, we detected a significant low enrichment of hnRNP F/H, using the mutant version of *LINC00672* in the pull-down assays followed by Western blotting, when the ~125-nt ultraconserved sequence was depleted (Fig. 5G). The results indicated that the 125-nt ultraconserved region of *LINC00672* may be a major hnRNP F/H-binding domain and that it is required for this association. To further confirm this interaction, we examined this interaction between *LINC00672* and hnRNP F/H by using RNA immunoprecipitation (RIP). The results showed a significant enrichment of *LINC00672* bound to the hnRNP F and H antibody, compared with the nonspecific IgG control antibody (Fig. 5, *H* and *I*). It is notable that we did not detect a direct interaction between *LINC00672* and p53 (Fig. 5, *H* and *I*). Taken together, these results demonstrated a specific association between hnRNP F/H and *LINC00672*.

LINC00672 recruits hnRNPs to promote p53-dependent suppression of *LASP1*

We next addressed the mechanism by which *LINC00672* suppresses *LASP1* expression. As p53 has been documented to directly suppress *LASP1* (21, 22), we cloned the proximal promoter region of *LASP1* to construct reporter plasmid (pGL3-*LASP1*), as well as another plasmid pGL3-*LASP1*Δp53RE with

the conserved p53 response elements (p53RE) depleted, and we further performed luciferase assays with inhibition of p53 or not. The pGL3-*LASP1* luciferase activities were increased by ~1.8-fold in the p53-inhibited EC cells (supplemental Fig. 2, *A* and *B*). As for the plasmid of pGL3-*LASP1*Δp53RE, no significant differences were detected in p53-inhibited EC cell lines (Fig. 6, *A* and *B*). However, several transcriptional co-activators, such as hnRNP K, have been implicated in the regulation of p53 target gene expression; this regulation occurs via the recruitment of p53 and/or via the stabilization of p53 binding (23, 24). Like previous studies that have discovered direct associations between lincRNA and hnRNPs (25–29), we speculated that *LINC00672* may also act as a cofactor of hnRNPs at the promoter of *LASP1*.

Consistent with previous data, we detected hnRNPs (including hnRNP F, H, K, D, and I) and p53 at the sites near the *LASP1* promoter, including p53REs (Fig. 6C), *LINC00672* overexpression, *LINC00672* mutant, and *LINC00672* knockdown, respectively, and the control cells via CHIP experiments (Fig. 6, *D* and *E*). Interestingly, we observed significant enrichments of hnRNP K, hnRNP F, hnRNP H, and p53 at the p53RE regions of the *LASP1* promoter in the cells that were transfected with *LINC00672* but not in the cells with *LINC00672* knockdown. The CHIP data also revealed that the binding of hnRNP K, F, H,

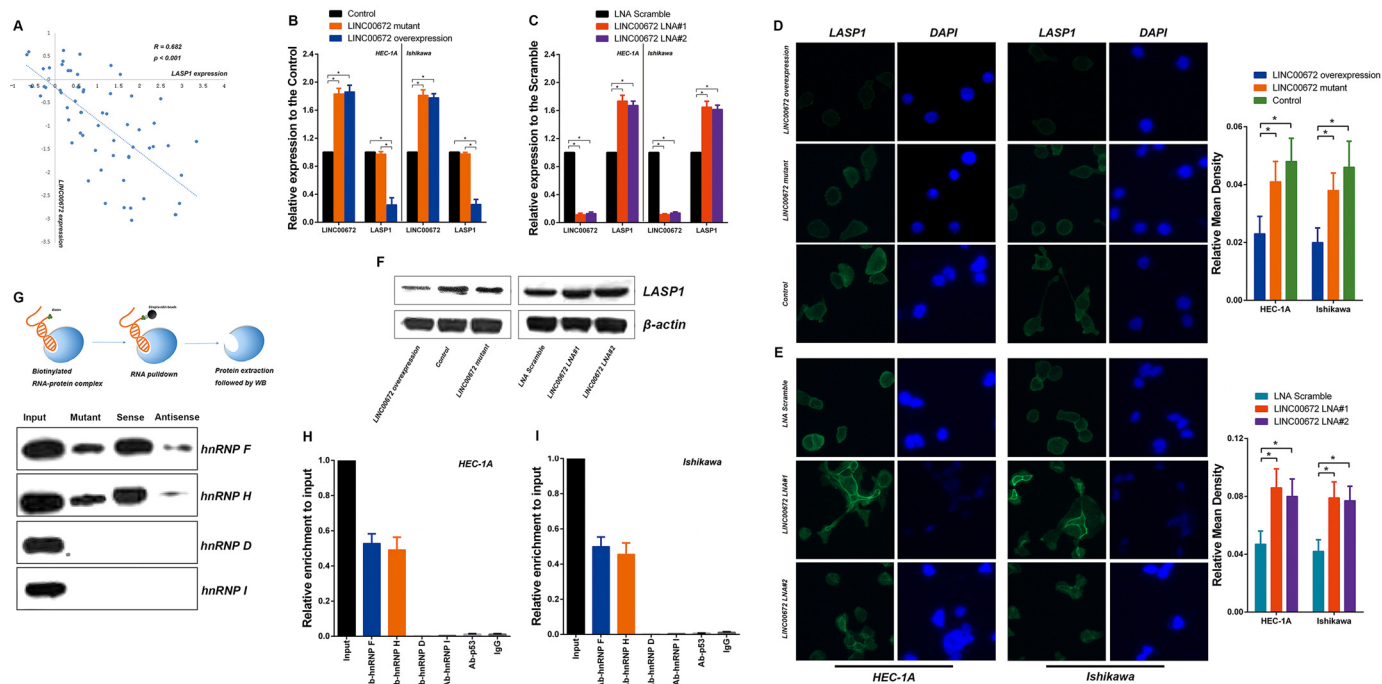


Figure 5. LINC00672 contributes to the p53-dependent *LASP1* suppression. *A*, association between log₂-transformed *LINC00672* and *LASP1* expression in a set of randomly selected 62 EC tumor and paired adjacent non-neoplastic tissues. *B*, *LINC00672* and *LASP1* expression levels detected by qPCR in EC cells after transfection with *LINC00672*, *LINC00672*-mutant, and control lentiviruses. Data shown are the mean \pm S.D. of three independent experiments, normalized to *GAPDH* (*, $p < 0.05$). *C*, *LINC00672* and *LASP1* expression levels detected by qPCR in EC cells after transfection with *LINC00672* LNA#1, *LINC00672* LNA#2 and LNA scramble. Data shown are the mean \pm S.D. of three independent experiments, normalized to *GAPDH* (*, $p < 0.05$). *D*, immunofluorescence analysis of *LASP1* in EC cells after transfection with *LINC00672*, *LINC00672*-mutant, and control lentiviruses. *Right panel* is the quantification of relative fluorescence mean density ($n = 6$, *, $p < 0.05$). *E*, immunofluorescence analysis of *LASP1* in EC cells after transfection with *LINC00672* LNA#1, *LINC00672* LNA#2, and LNA scramble. *Right panel* is the quantification of relative fluorescence mean density ($n = 6$, *, $p < 0.05$). *F*, *LASP1* levels in HEC-1A cells detected by Western blotting after transfection with *LINC00672* lentiviruses, *LINC00672*-mutant lentiviruses, control lentiviruses, *LINC00672* LNA#1, *LINC00672* LNA#2, and LNA scramble. *G*, schema of RNA pull-down experiment followed by Western blotting for verification of hnRNP F/H association (upper). Western blotting results of hnRNP F, H, D, and I in the protein extractions of *LINC00672*-pull-down are shown. *H* and *I*, RIP experiments were performed using hnRNP F, H, D, and I and p53 antibody to immunoprecipitate and a primer to detect *LINC00672* in HEC-1A and Ishikawa cells.

and p53 at the *LASP1* p53REs was reduced to the control levels in the *LINC00672*-mutant cells (Fig. 6, *D* and *E*), indicating that *LINC00672* may be required for the recruitment of hnRNP F, H, K, and p53 to the p53REs of the *LASP1* promoter. Moreover, the strength of p53 binding at the *LASP1* promoter was significantly diminished in the *LINC00672*-knockdown cells and elevated in the *LINC00672*-overexpression cells, but no significant changes were shown in the *LINC00672*-mutant cells (Fig. 6*D*).

Consistent with the model wherein *LINC00672*, hnRNP F, H, and K cooperate to assist p53-dependent repression of *LASP1* transcription, the knockdown of hnRNP F, H, and K lowered p53 enrichment at the p53RE regions of *LASP1* in EC cells (Fig. 6*F* and supplemental Fig. 2, *I* and *J*). Furthermore, the previous reported that hnRNP F could directly interacted with hnRNP K (30) was also confirmed by our co-immunoprecipitation assays (supplemental Fig. 2*K*).

To test whether *LINC00672* was required to guide hnRNP K, F, H, and p53 to the *LASP1* promoter, we transfected EC cells with biotin-labeled *LINC00672* and captured *LINC00672*-associated DNA with streptavidin-coated beads. The associated *LASP1* sequence overlapped with the 5' end of the p53RE region of *LASP1* (amplicons 2 and 3), whereas the upstream or downstream regions (amplicons 1, 4, and 5) were not bound (Fig. 6*G*). These results suggested that *LINC00672* RNA is required for the recruitment of p53 and its cofactors to the

p53REs of the promoter of *LASP1* and for the efficient p53 binding at this sites.

Ectopic *LINC00672* expression influences paclitaxel IC_{50} in vitro and paclitaxel chemosensitivity in vivo

All the EC patients were classified into groups according to the FIGO stage classification criteria. We observed that *LINC00672* and *LASP1* expression modestly correlated with the FIGO stages. The patients of stage I expressed a higher level of *LINC00672* than the patients of stages II and III, whereas *LASP1* expression was higher in the patients of stage III than the patients of stages I and II (Fig. 7, *A–C*).

To investigate the impact of *LINC00672* on the chemotherapeutic effect, we calculated the 50% maximal inhibitory concentration (IC_{50}) of paclitaxel, carboplatin, and cisplatin in *LINC00672* overexpression, *LINC00672* mutant, and *LINC00672* knockdown, respectively, and control EC cells. The estimated IC_{50} of paclitaxel significantly decreased when *LINC00672* was overexpressed, whereas *LINC00672* knockdown markedly increased the paclitaxel IC_{50} of EC cells. However, the paclitaxel IC_{50} of the *LINC00672*-mutant cells showed no significant difference in the WT cells (Fig. 7*D*). We observed no significant influence on the tolerance of carboplatin and cisplatin in the EC cells with different *LINC00672* expression (Fig. 7, *E* and *F*).

LINC00672 and endometrial cancer

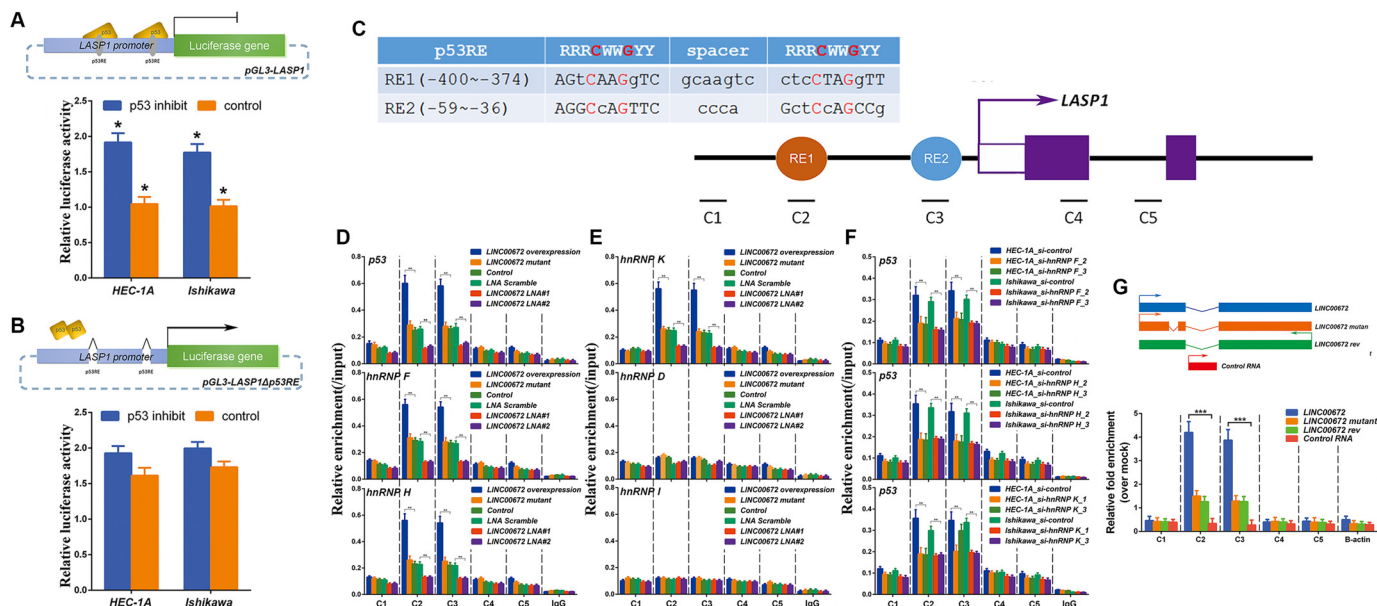


Figure 6. LINC00672 recruits hnRNPs to promote p53-dependent *LASP1* suppression. *A* and *B*, luciferase reporter assay in HEC-1A and Ishikawa cells with p53 pharmacologically inhibited or not. The reporter constructs expressing the luciferase gene under *LASP1* gene promoter or the p53RE-deficient *LASP1* promoter segment. Data are presented as the mean \pm S.E. ($n = 3$, $p < 0.05$). *C*, illustration of two putative p53 response elements (RE1, red; RE2, blue) found in the *LASP1* TSS. The positions relative to the *LASP1* TSS are indicated by numbers. The alignment between the well defined consensus p53-binding site ($R = A/G$, $W = A/T$, and $Y = C/T$) and the sequence of the two putative sites are shown, with the strictly conserved C/G highlighted in red. *D* and *E*, ChIP assays showing the enrichment of p53, hnRNP F, H, K, D, and I at *LASP1* in HEC-1A cells transfected with *LINC00672* lentiviruses, *LINC00672*-mutant lentiviruses, control lentiviruses, *LINC00672* LNA#1, *LINC00672* LNA#2, and LNA scramble. Co-precipitated DNA was analyzed by qPCR using amplicons C1–C5. Data are represented as means \pm S.E. ($n = 3$, $p < 0.05$). *F*, chromatin immunoprecipitation assays showing the enrichment of p53 at *LASP1* in HEC-1A and Ishikawa cells transfected with HNRNPF_sirRNAs, HNRNPH_sirRNAs, HNRNPK_sirRNAs, or control RNAs. Co-precipitated DNA was analyzed by qPCR using amplicons C1–C5. Data are represented as mean \pm S.E. of three independent experiments ($n = 3$, $p < 0.05$). *G*, DNA capture assay using HEC-1A cells transfected with biotinylated RNAs shown above. Biotinylated RNA was captured with streptavidin-coated beads, and associated *LASP1* DNA (amplicons 1–5) was analyzed by qPCR. Data are represented as mean \pm S.E. of three independent experiments ($n = 3$, $p < 0.05$).

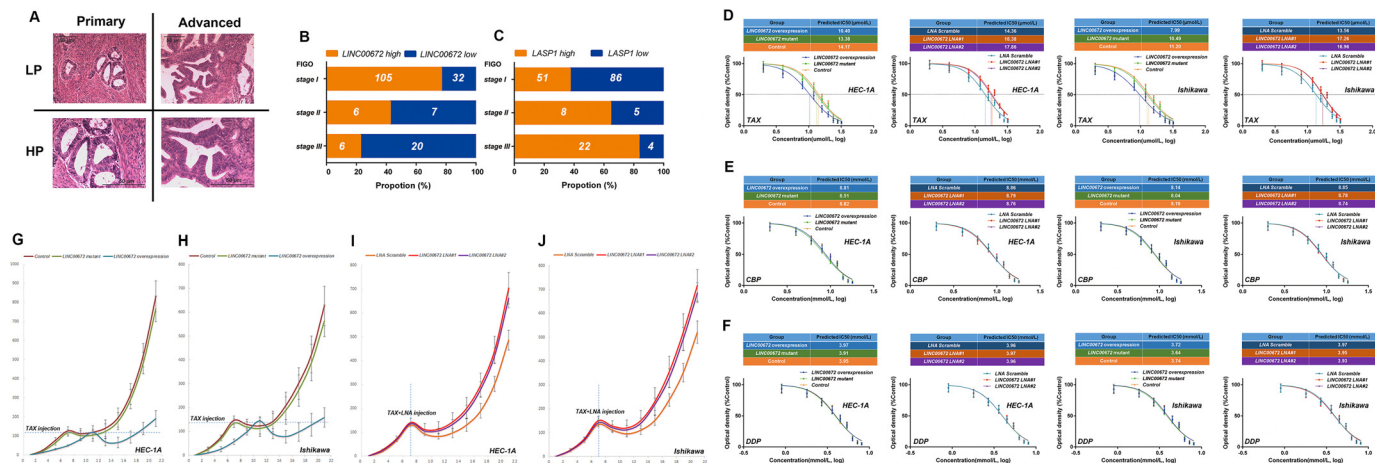


Figure 7. LINC00672 increases the paclitaxel chemosensitivity of EC *in vitro* and *in vivo*. *A*, pathologic sections of primary and advanced endometrial carcinoma. *L.P.*, low power lens; *HIP.*, high power lens. *B* and *C*, *LINC00672* and *LASP1* expression patterns in all endometrial carcinoma samples classified by FIGO stages. The expression level was analyzed by qRT-PCR and normalized to *GAPDH*. The high and low classes were determined by median expression level. *D–F*, 50% inhibitory concentration of paclitaxel (TAX), carboplatin (CBP), cisplatin (DIP), on HEC-1A and Ishikawa cells after transfection with *LINC00672* lentiviruses, *LINC00672*-mutant lentiviruses, control lentiviruses, *LINC00672* LNA#1, *LINC00672* LNA#2, and LNA scramble. *G* and *H*, paclitaxel therapy effects on xenograft mice subcutaneously implanted with *LINC00672*-up-regulated, *LINC00672*-mutant, and respective control EC cells. Each point represents the mean tumor volume. Bars, S.E. Mean tumor volumes from six nude mice of each group are shown ($p < 0.05$). *I* and *J*, paclitaxel therapy effects on xenograft mice intraperitoneally injected with *LINC00672* LNA#1, *LINC00672* LNA#2, and LNA scramble. Each point represents the mean tumor volume. Bars, S.E. Mean tumor volumes from six nude mice of each group are shown ($p < 0.05$).

To verify whether those *in vitro* observations of *LINC00672* impact the paclitaxel chemosensitivity of EC cells can be extended to the response of EC xenograft mouse model *in vivo*, individual animals hypodermic injection with *LINC00672*-manipulated EC cells (stably expressed *LINC00672* and

LINC00672 mutant), and control cells were treated with a specific dose of paclitaxel (12.5 mg/kg, intraperitoneally (i.p.)) at the check points when each xenograft tumor size reaches the injection line (about 120 mm³). We observed that EC xenograft with overexpressed *LINC00672* exhibited a greater amount of

paclitaxel sensitivity, whereas there was no difference in the growth path of xenograft tumor in response to the paclitaxel treatment between the EC cells transfected with defective *LINC00672* and the control cells (Fig. 7, *G* and *H*). To explore the impact of *LINC00672* knockdown on paclitaxel sensitivity, we intraperitoneally injected *in vivo* optimized *LINC00672*-targeting LNAs (16 mg/kg) and paclitaxel (12.5 mg/kg) into individual mice on day 7 after the hypodermic injection in wild-type EC cells was completed. We observed a strongly induced tolerance (after injecting *LINC00672* LNAs) in response to paclitaxel treatment in EC xenograft mice (Fig. 7, *I* and *J*). Moreover, Ki67 immunostaining showed less proliferation in xenograft tumors of the *LINC00672*-overexpressed EC cells, and TUNEL staining showed more apoptosis in *LINC00672*-overexpressed EC xenograft following paclitaxel injection (supplemental Fig. 2, *P–S*).

Discussion

In this study, we expanded our knowledge about the 26 previously reported lincRNAs (14), which show a high sequence and position conservation throughout evolution. We then examined their expression patterns in a large cohort of EC patients from two distinct population centers in China (12). We found that of the 13 candidate lincRNAs, *LINC00672* was significantly down-regulated in human EC tissues and that the expression pattern of *LINC00672* is associated with EC FIGO stages. These data suggest that *LINC00672* contributes to important biologic functions in cellular biology and oncogenesis (5–7, 31–34).

LINC00672 is a 2365-bp transcript with two exons located in the forward strand of chromosome 17q12, an EC susceptibility locus, which is associated with prostate cancer, breast cancer, and type 2 diabetes (35, 36). Interestingly, our *in vitro* and *in vivo* experiments, along with the data of a previous study of p53 transcription regulation (18), suggest that *LINC00672* might be a novel p53 transcriptional target. *LINC00672*, as reported previously (12, 14), is a member of a small category of lincRNA orthologs found in non-mammals. Our investigation showed that *LINC00672* possesses a detectable sequence conservation and is restricted to a single short region of ultra-conservation. Furthermore, its genomic location is conserved: it is always adjacent to the *LASPI* gene in the tandem downstream orientation. Moreover, along with the low single-cell copy number (~60 molecules/cell), the overexpression of *LINC00672* could drive the down-regulation of the *LASPI* gene in EC cells, whereas deficient *LINC00672* overexpression induced no changes. These data led us to believe that the contribution of *LINC00672* to cellular biology and oncogenesis may be associated, at least in part, with *LASPI*.

LASPI is overexpressed and associated with increased tumor aggressiveness in numerous types of cancers (37–40), suggesting that *LASPI* levels may serve as a prognostic marker. Not only is *LASPI* regulated by miRNAs, it is a *bona fide* target of repression of the tumor suppressor p53 (21, 22). Because it is also involved in cytoskeletal organization and cell motility (41, 42), the knockdown of *LASPI* often leads to the decreased migration and proliferation of human cancer cells (43–48). Our data revealed that *LINC00672* overexpression reduced the pro-

liferation, migration, and invasion of the EC cells and their ability to form colonies and to establish xenografts. The knockdown of *LASPI* could rescue the impact of *LINC00672* on the proliferation and migration of the EC cells (supplemental Fig. 2, *L–O*). Our mechanistic experimental data suggested that *LINC00672* functioned as a cofactor in concert with hnRNPs to facilitate p53-dependent *LASPI* suppression. Therefore, it is associated with the aggression and malignancy of EC.

Compared with other gynecologic malignancies, EC exhibits relatively poor chemosensitivity. Although paclitaxel, despite its toxicity, is the primary single chemotherapeutic agent for the treatment of advanced or recurrent EC, an increase in the sensitivity of EC cells to paclitaxel is an essential strategy to improve its chemotherapeutic effect on EC patients. Paclitaxel binds to the α -tubulin subunit and stabilizes the cytoskeleton, resulting in the disruption of normal microtubule dynamics (49). As a cytoskeleton-regulatory protein, the *LASPI* level appeared to be up-regulated in induced paclitaxel-resistant human cancer cells. Therefore, the overexpression of *LINC00672* could lower the paclitaxel IC₅₀ and promote the chemosensitivity of EC cells *in vitro* and *in vivo*. Moreover, wild-type p53 is known to contribute to tumor growth and sensitize cancer cells to chemotherapeutic drugs (50), whereas hnRNP H also plays a role in the promotion of the paclitaxel sensitivity of EC cells. Collectively, these findings and our data suggest that *LINC00672* participates in the p53-mediated suppression of *LASPI* via its interaction with hnRNPs and that this participation may have potential clinical value for EC chemotherapy (Fig. 8).

In summary, this study represents a large analysis of EC samples of different stages for the expression of *LINC00672*, which is significantly down-regulated in EC tumor tissues. The overexpression of *LINC00672* reduces the migration and proliferation of EC cells. These anti-tumor effects of *LINC00672* relate at least partially to its cooperation with hnRNPs during p53-mediated *LASPI* suppression. Thus, *LINC00672* could promote paclitaxel chemosensitivity of EC cells. Overall, our findings elucidate the orchestrated function of lincRNAs that serve as conserved position markers when they participate in canonical transcriptional regulatory processes and thereby play crucial roles for EC initiation and progression.

Experimental procedures

Human study subjects

104 fresh EC tissues and paired adjacent non-cancerous tissue samples were obtained from the patients in eastern China who underwent hysterectomies at the Affiliate Hospitals of Soochow University (Suzhou). Seventy two fresh EC tissues were collected from the patients at the Cancer Hospitals affiliated with Guangzhou Medical University in southern China and were used for further validation. None of the patients received anti-cancer treatment before surgery, including chemotherapy or radiotherapy. This study was approved by the Medical Ethics Committees of Soochow University and Guangzhou Medical College. The clinical characteristics of the patients are listed in supplemental Table 1.

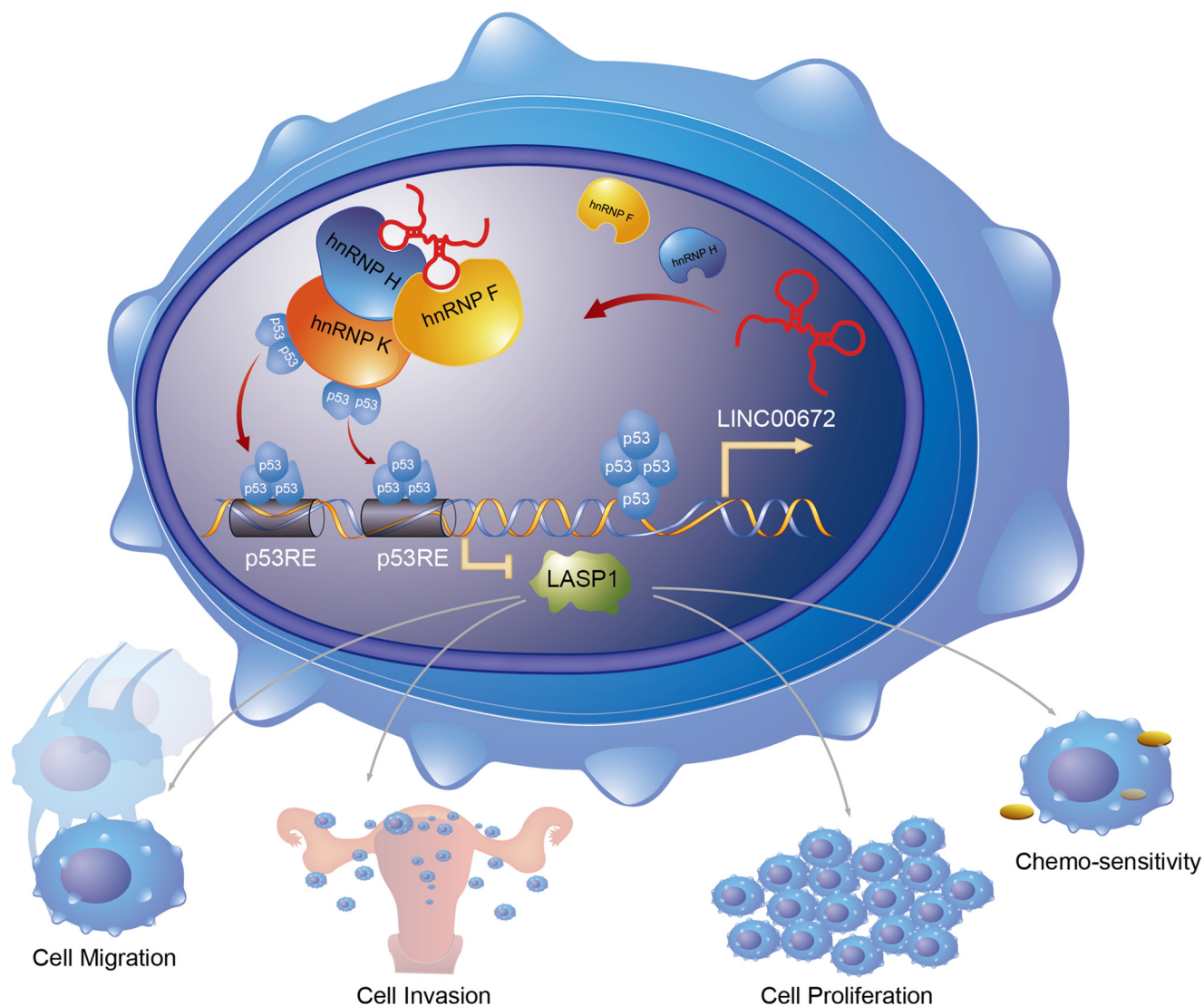


Figure 8. Model depicting the role of *LINC00672* in the p53-dependent regulation of *LASP1*. *LINC00672* participates in the p53-mediated suppression of *LASP1* via its interaction with hnRNPs. p53 could regulate *LINC00672* transcription from *LASP1* gene locus and then *LINC00672* recruits hnRNP F/H and hnRNP K, guiding p53 binds to the p53RE of *LASP1*, forming a p53 regulation loop.

Evolutionary conventional lincRNA screening

We confirmed and categorized the previously reported 26 lincRNAs (14) in the UCSC, Ensembl, Refseq, Vega, and ENCODE databases. Only 13 lincRNAs that were confirmed by these genome databases were selected as our candidates (supplemental Table 2).

Cell lines and p53^{-/-} mice

The human EC cell lines HEC-1A, Ishikawa, and the embryonic kidney cell line 293T were purchased from Cell Bank of Chinese Academy of Sciences. All cell lines passaged for fewer than 6 months and characterized by DNA fingerprinting analysis were maintained and used in this study. The p53^{-/-} mice (The Jackson Laboratory, stock number 002101) were provided by the Biomedical Research Institute of Nanjing University.

Xenograft growth and analysis of paclitaxel chemosensitivity of EC in mice

A total of 0.1 ml of cell suspension (1×10^6 /ml) was injected subcutaneously into the hind flanks of the mice. Mice were then

intraperitoneally injected with paclitaxel (12.5 mg/kg; Mayne Pharma, Australia). For animal study with LNA injection, mice were intraperitoneally injected with *in vivo*-grade LNAs (Exiqon) in PBS (15 mg/kg) and paclitaxel at day 7 after subcutaneous injection into EC cells.

RNA extraction and quantitative real time PCR analysis

Total RNA from the endometrial tissue specimens and from cells were extracted with TRIzol reagent (Invitrogen). First-strand cDNA was synthesized with the Superscript II-reverse transcriptase kit (Invitrogen). All qRT-PCR primers are listed in supplemental Table 3.

Cell fractionation

Cells were resuspended in buffer 1 for 10 min on ice. After a centrifugation at $300 \times g$ for 2 min, the supernatant was collected as the cytoplasmic fraction. Then the pellet was resuspended in buffer 2 for 10 min on ice. Chromatin was pelleted at maximum speed for 3 min. The supernatant represents the nuclear fraction.

Northern blotting

LINC00672 Northern blotting was performed using a DIG Northern Starter Kit (Roche Applied Science, Germany) following the manufacturer's instructions. A total of 10 μg of the indicated RNA was subjected to formaldehyde gel electrophoresis and transferred to a Biotinyne nylon membrane (Pall, NY). The PCR primers were designed against the 125-nt ultraconserved region and listed in supplemental Table 3.

5'- and 3'-Rapid amplification of cDNA ends

5' - and 3' -RACE was used to determine the transcriptional initiation and termination sites of LINC00672 using a SMARTerTM RACE cDNA amplification kit (Clontech).

RNA pulldown assay

Biotinylated LINC00672 or its antisense RNA was incubated with cellular protein extracts, which were then treated with streptavidin beads. Recovered proteins that associated with LINC00672 were resolved by gel electrophoresis. The band of interest was excised and analyzed by mass spectrometry.

RNA immunoprecipitation

We performed RNA immunoprecipitation (RIP) experiments using a Magna RIP kit (Millipore, Bedford, MA) following the manufacturer's instructions. The hnRNP F/H antibody used for RIP was clone ab10689 (Abcam, Shanghai, China).

DNA capture assay

Cells were transfected with biotinylated LINC00672, fixed, and then lysed. Chromatin was sheared by sonication, and the supernatant was incubated with streptavidin-coated magnetic beads (Pierce, Thermo Fisher Scientific). RNA was isolated, and RNA-associated DNA was quantified by qPCR (supplemental Table 3).

Plasmids, lentiviral production, siRNA, and LNA

The full-length human LINC00672 cDNA and the defective version that lacked the conserved regions were synthesized by GeneWiz (Beijing, China) and cloned into the lentiviral expression vector pLVX-IRES-neo (Clontech) (51). siRNAs targeting *LASPI*, *hnRNP K*, *F*, and *H* from Genepharma (Shanghai, China) were used in this study. The knockdown efficiency and specificity of all siRNAs were validated with qPCR. LNAs targeting LINC00672 or a scrambled sequence were designed (LNA#1: 590579-1; LNA#2: 590579-2; LNA#3: 590579-3) and synthesized from Exiqon.

Construction of reporter plasmids, transient transfections, and luciferase assays

The evolutionarily conserved enhancer and the binding motif that are regulated by p53 have been previously identified in the *LASPI* gene (52). The fragment was synthesized and then inserted into the pGL3-basic vector (Promega, Madison, WI) (termed the pGL3-*LASPI* promoter). Another plasmid termed pGL3-*LASPIN* promoter was the deficient version, in which the binding motif was deleted from the pGL3-*LASPI* promoter. Finally, all constructs were sequenced to verify the allele, orientation, and integrity of each insert.

Pharmacologic inhibition of p53 and Western blotting

To pharmacologically inhibit p53, cells were treated with either 0.1 μM pifithrin- α or DMSO (vehicle control). For Western blotting, the samples were incubated overnight at 4 °C with either an anti-p53 antibody (Abcam, ab179477) or an anti- β -actin antibody (Abcam, ab8226).

Chromatin immunoprecipitation

ChIP assays were performed with an EZ-ChIP kit (Millipore, Bedford, MA) following the manufacturer's instructions. Chromatin from EC cells was immunoprecipitated with antibodies against hnRNP K (ab39975, Abcam), hnRNP F (ab50982, Abcam), hnRNP H (ab10374, Abcam), p53(ab179477, Abcam), and IgG control (sc-2027, Santa Cruz Biotechnology) (supplemental Table 3).

Western blotting and immunocytochemistry

Protein lysates from EC cells were subjected to a Western blotting analysis with anti-LASPI (ab117806, Abcam), anti-p53 (ab179477, Abcam), anti-hnRNP K (ab39975, Abcam), hnRNP F(ab50982, Abcam), hnRNP H(ab10374, Abcam), and anti-actin β (Abcam, ab8226) antibodies according to standard protocols as described previously (53). An immunofluorescence analysis of *LASPI* was performed using an immunofluorescence staining kit (Beyotime Institute of Biotechnology, China) following the manufacturer's instructions.

Flow cytometry analysis of apoptosis, xenograft, TUNEL, and Ki67 staining

For apoptosis analysis, annexin V-FITC/PI staining was performed by using flow cytometry according to the manufacturer's guidelines (Roche Applied Science, Germany). Xenograft tumors were collected on day 16. The levels of proliferation and cell survival in the xenograft tissues were detected by Ki67 immunostaining and TUNEL staining according to the manufacturer's instructions (Roche Applied Science, Germany).

Analysis of cell proliferation, cell cycle, wound healing, and colony formation ability

For cell viability, cells were seeded in 96-well flat-bottomed plates and then measured with a CCK-8 assay (Dojindo, Japan). For cell cycle, cells fixed in 70% ethanol and labeled with PI (Sigma) were then analyzed by flow cytometry (Beckman Coulter). For wound-healing assay, cells were treated with mitomycin C, grown to confluence as a monolayer, and then wounded with a 10- μl pipette tip in non-serum medium. For colony formation assay, cells were seeded in 65-mm culture dishes and were allowed to grow until visible colonies formed (2 weeks). All experiments were repeated at least three times.

Transwell migration and Matrigel invasion assays

The ability of the cells to migrate and invade was assessed using Corning Transwell insert chambers with pores 8 mm in size (Corning) and a BioCoat Matrigel Invasion Chamber (BD Biosciences), respectively. Approximately 1×10^4 (migration assay) or 2×10^5 (invasion assay) transfected cells in 200 μl of serum-free RPMI 1640 medium were seeded in the upper well;

the chambers were then incubated with RPMI 1640 medium plus 20% fetal bovine serum for 48 h at 37 °C to allow the cells to migrate to the lower well. The cells that had migrated or invaded through the membrane were fixed in methanol, stained with crystal violet (Invitrogen), imaged, and counted.

Paclitaxel IC₅₀

Cells were seeded in 96-well plates (1×10^4 cells per well) and incubated for 48 h with various concentrations (2×10^{-6} to 3.2×10^{-5} M) of paclitaxel, (2×10^{-3} to 1.8×10^{-2} M) of carboplatin, and (9×10^{-4} to 8.1×10^{-3} M) of cisplatin. The IC₅₀ of each cell line was calculated with the SigmaPlot software (Systat Software, Point Richmond, CA).

Statistical analysis

One-way analysis of variance tests were used to investigate the effect of altered *LINC00672* expression on the *LASPI* mRNA levels in EC cells. Linear regression models were used to examine the correlation between the expression of *LINC00672* and the expression of the *LASPI* gene in EC tissues. A rank-sum test was used to identify the *LINC00672* expression pattern in the EC patients of each FIGO stage. The differences among the groups were assessed with a paired two-tailed Student *t* test. $p < 0.05$ was considered significant. The ribosome profiling data were obtained from Gene Expression Omnibus (accession no. GSE61742).

Author contributions—W. L., H. L., and Y. Z. contributed to the conception, design, and writing of the paper. W. L., H. L., L. Z., and F. L. designed, performed, and analyzed the experiments. M. H., J. D., M. A., S. W., R. M., and J. L. performed and analyzed the data.

References

1. Ferlay, J., Shin, H. R., Bray, F., Forman, D., Mathers, C., and Parkin, D. M. (2010) Estimates of worldwide burden of cancer in 2008: GLOBOCAN 2008. *Int. J. Cancer* **127**, 2893–2917
2. Montesano, R., Hollstein, M., and Hainaut, P. (1996) Genetic alterations in esophageal cancer and their relevance to etiology and pathogenesis: a review. *Int. J. Cancer* **69**, 225–235
3. Guttman, M., Amit, I., Garber, M., French, C., Lin, M. F., Feldser, D., Huarte, M., Zuk, O., Carey, B. W., Cassady, J. P., Cabili, M. N., Jaenisch, R., Mikkelsen, T. S., Jacks, T., Hacohen, N., *et al.* (2009) Chromatin signature reveals over a thousand highly conserved large non-coding RNAs in mammals. *Nature* **458**, 223–227
4. Khalil, A. M., Guttman, M., Huarte, M., Garber, M., Raj, A., Rivea Morales, D., Thomas, K., Presser, A., Bernstein, B. E., van Oudenaarden, A., Regev, A., Lander, E. S., and Rinn, J. L. (2009) Many human large intergenic noncoding RNAs associate with chromatin-modifying complexes and affect gene expression. *Proc. Natl. Acad. Sci. U.S.A.* **106**, 11667–11672
5. Gupta, R. A., Shah, N., Wang, K. C., Kim, J., Horlings, H. M., Wong, D. J., Tsai, M. C., Hung, T., Argani, P., Rinn, J. L., Wang, Y., Brzoska, P., Kong, B., Li, R., West, R. B., *et al.* (2010) Long non-coding RNA HOTAIR reprograms chromatin state to promote cancer metastasis. *Nature* **464**, 1071–1076
6. Huarte, M., Guttman, M., Feldser, D., Garber, M., Koziol, M. J., Kenzelmann-Broz, D., Khalil, A. M., Zuk, O., Amit, I., Rabani, M., Attardi, L. D., Regev, A., Lander, E. S., Jacks, T., and Rinn, J. L. (2010) A large intergenic noncoding RNA induced by p53 mediates global gene repression in the p53 response. *Cell* **142**, 409–419
7. Ørom, U. A., Derrien, T., Beringer, M., Gumireddy, K., Gardini, A., Busotti, G., Lai, F., Zytynicki, M., Notredame, C., Huang, Q., Guigo, R., and Shiekhattar, R. (2010) Long noncoding RNAs with enhancer-like function in human cells. *Cell* **143**, 46–58
8. Guttman, M., Donaghey, J., Carey, B. W., Garber, M., Grenier, J. K., Munson, G., Young, G., Lucas, A. B., Ach, R., Bruhn, L., Yang, X., Amit, I., Meissner, A., Regev, A., Rinn, J. L., *et al.* (2011) lincRNAs act in the circuitry controlling pluripotency and differentiation. *Nature* **477**, 295–300
9. Faghihi, M. A., Modarresi, F., Khalil, A. M., Wood, D. E., Sahagan, B. G., Morgan, T. E., Finch, C. E., St Laurent G., 3rd, Kenny, P. J., and Wahlestedt, C. (2008) Expression of a noncoding RNA is elevated in Alzheimer's disease and drives rapid feed-forward regulation of β -secretase. *Nat. Med.* **14**, 723–730
10. Qureshi, I. A., Mattick, J. S., and Mehler, M. F. (2010) Long non-coding RNAs in nervous system function and disease. *Brain Res.* **1338**, 20–35
11. Yu, W., Gius, D., Onyango, P., Muldoon-Jacobs, K., Karp, J., Feinberg, A. P., and Cui, H. (2008) Epigenetic silencing of tumour suppressor gene p15 by its antisense RNA. *Nature* **451**, 202–206
12. Li, W., Zheng, J., Deng, J., You, Y., Wu, H., Li, N., Lu, J., and Zhou, Y. (2014) Increased levels of the long intergenic non-protein coding RNA POU3F3 promote DNA methylation in esophageal squamous cell carcinoma cells. *Gastroenterology* **146**, 1714–1726
13. Guttman, M., Garber, M., Levin, J. Z., Donaghey, J., Robinson, J., Adiconis, X., Fan, L., Koziol, M. J., Gnirke, A., Nusbaum, C., Rinn, J. L., Lander, E. S., and Regev, A. (2010) *Ab initio* reconstruction of cell type-specific transcripts in mouse reveals the conserved multi-exonic structure of lincRNAs. *Nat. Biotechnol.* **28**, 503–510
14. Ulitsky, I., Shkumatava, A., Jan, C. H., Sive, H., and Bartel, D. P. (2011) Conserved function of lincRNAs in vertebrate embryonic development despite rapid sequence evolution. *Cell* **147**, 1537–1550
15. Wang, K. C., Yang, Y. W., Liu, B., Sanyal, A., Corces-Zimmerman, R., Chen, Y., Lajoie, B. R., Protacio, A., Flynn, R. A., Gupta, R. A., Wysocka, J., Lei, M., Dekker, J., Helms, J. A., and Chang, H. Y. (2011) A long noncoding RNA maintains active chromatin to coordinate homeotic gene expression. *Nature* **472**, 120–124
16. Battle, A., Khan, Z., Wang, S. H., Mitrano, A., Ford, M. J., Pritchard, J. K., and Gilad, Y. (2015) Genomic variation. Impact of regulatory variation from RNA to protein. *Science* **347**, 664–667
17. Guttman, M., Russell, P., Ingolia, N. T., Weissman, J. S., and Lander, E. S. (2013) Ribosome profiling provides evidence that large noncoding RNAs do not encode proteins. *Cell* **154**, 240–251
18. Sánchez, Y., Segura, V., Marín-Béjar, O., Athie, A., Marchese, F. P., González, J., Bujanda, L., Guo, S., Matheu, A., and Huarte, M. (2014) Genome-wide analysis of the human p53 transcriptional network unveils a lincRNA tumour suppressor signature. *Nature communications* **5**, 5812
19. Tsai, M. C., Manor, O., Wan, Y., Mosammaparast, N., Wang, J. K., Lan, F., Shi, Y., Segal, E., and Chang, H. Y. (2010) Long noncoding RNA as modular scaffold of histone modification complexes. *Science* **329**, 689–693
20. Bellucci, M., Agostini, F., Masin, M., and Tartaglia, G. G. (2011) Predicting protein associations with long noncoding RNAs. *Nat. Methods* **8**, 444–445
21. Wang, B., Feng, P., Xiao, Z., and Ren, E. C. (2009) LIM and SH3 protein 1 (Lasp1) is a novel p53 transcriptional target involved in hepatocellular carcinoma. *J. Hepatol.* **50**, 528–537
22. Wang, B., Xiao, Z., and Ren, E. C. (2009) Redefining the p53 response element. *Proc. Natl. Acad. Sci. U.S.A.* **106**, 14373–14378
23. Jung, Y. S., Qian, Y., and Chen, X. (2010) Examination of the expanding pathways for the regulation of p21 expression and activity. *Cell. Signal.* **22**, 1003–1012
24. Moumen, A., Masterson, P., O'Connor, M. J., and Jackson, S. P. (2005) hnRNP K: an HDM2 target and transcriptional coactivator of p53 in response to DNA damage. *Cell* **123**, 1065–1078
25. Dimitrova, N., Zamudio, J. R., Jong, R. M., Soukup, D., Resnick, R., Sarma, K., Ward, A. J., Raj, A., Lee, J. T., Sharp, P. A., and Jacks, T. (2014) LincRNA-p21 activates p21 in cis to promote Polycomb target gene expression and to enforce the G1/S checkpoint. *Mol. Cell* **54**, 777–790
26. Huang, J., Zhou, N., Watabe, K., Lu, Z., Wu, F., Xu, M., and Mo, Y. Y. (2014) Long non-coding RNA UCA1 promotes breast tumor growth by suppression of p27 (Kip1). *Cell Death Dis.* **5**, e1008

27. Gumireddy, K., Li, A., Yan, J., Setoyama, T., Johannes, G. J., Orom, U. A., Tchou, J., Liu, Q., Zhang, L., Speicher, D. W., Calin, G. A., and Huang, Q. (2013) Identification of a long non-coding RNA-associated RNP complex regulating metastasis at the translational step. *EMBO J.* **32**, 2672–2684
28. Carpenter, S., Aiello, D., Atianand, M. K., Ricci, E. P., Gandhi, P., Hall, L. L., Byron, M., Monks, B., Henry-Bezy, M., Lawrence, J. B., O'Neill, L. A., Moore, M. J., Caffrey, D. R., and Fitzgerald, K. A. (2013) A long noncoding RNA mediates both activation and repression of immune response genes. *Science* **341**, 789–792
29. Kumar, P. P., Emechebe, U., Smith, R., Franklin, S., Moore, B., Yandell, M., Lessnick, S. L., and Moon, A. M. (2014) Coordinated control of senescence by lncRNA and a novel T-box3 co-repressor complex. *eLife* **3**, e2805
30. Wei, C. C., Zhang, S. L., Chen, Y. W., Guo, D. F., Ingelfinger, J. R., Bomsztyk, K., and Chan, J. S. (2006) Heterogeneous nuclear ribonucleoprotein K modulates angiotensinogen gene expression in kidney cells. *J. Biol. Chem.* **281**, 25344–25355
31. Rinn, J. L., Kertesz, M., Wang, J. K., Squazzo, S. L., Xu, X., Bruggmann, S. A., Goodnough, L. H., Helms, J. A., Farnham, P. J., Segal, E., and Chang, H. Y. (2007) Functional demarcation of active and silent chromatin domains in human HOX loci by noncoding RNAs. *Cell* **129**, 1311–1323
32. Yap, K. L., Li, S., Muñoz-Cabello, A. M., Raguz, S., Zeng, L., Mujtaba, S., Gil, J., Walsh, M. J., and Zhou, M. M. (2010) Molecular interplay of the noncoding RNA ANRIL and methylated histone H3 lysine 27 by polycomb CBX7 in transcriptional silencing of INK4a. *Mol. Cell* **38**, 662–674
33. Wu, W., Bhagat, T. D., Yang, X., Song, J. H., Cheng, Y., Agarwal, R., Abraham, J. M., Ibrahim, S., Bartenstein, M., Hussain, Z., Suzuki, M., Yu, Y., Chen, W., Eng, C., Greal, J., et al. (2013) Hypomethylation of noncoding DNA regions and overexpression of the long noncoding RNA, AFAP1-AS1, in Barrett's esophagus and esophageal adenocarcinoma. *Gastroenterology* **144**, 956–966
34. Yang, X., Song, J. H., Cheng, Y., Wu, W., Bhagat, T., Yu, Y., Abraham, J. M., Ibrahim, S., Ravich, W., Roland, B. C., Khashab, M., Singh, V. K., Shin, E. J., Yang, X., Verma, A. K., Meltzer, S. J., and Mori, Y. (2014) Long non-coding RNA HNF1A-AS1 regulates proliferation and migration in oesophageal adenocarcinoma cells. *Gut* **63**, 881–890
35. Tomasetto, C., Régnier, C., Moog-Lutz, C., Mattei, M. G., Chenard, M. P., Lidereau, R., Basset, P., and Rio, M. C. (1995) Identification of four novel human genes amplified and overexpressed in breast carcinoma and localized to the q11-q21.3 region of chromosome 17. *Genomics* **28**, 367–376
36. Spurdle, A. B., Thompson, D. J., Ahmed, S., Ferguson, K., Healey, C. S., O'Mara, T., Walker, L. C., Montgomery, S. B., Dermitzakis, E. T., Australian National Endometrial Cancer Study Group, Fahey, P., Montgomery, G. W., Webb, P. M., Fasching, P. A., Beckmann, M. W., et al. (2011) Genome-wide association study identifies a common variant associated with risk of endometrial cancer. *Nat. Genet.* **43**, 451–454
37. Frietsch, J. J., Grunewald, T. G., Jasper, S., Kammerer, U., Herterich, S., Kapp, M., Honig, A., and Butt, E. (2010) Nuclear localisation of LASP-1 correlates with poor long-term survival in female breast cancer. *Br. J. Cancer* **102**, 1645–1653
38. Orth, M. F., Cazes, A., Butt, E., and Grunewald, T. G. (2015) An update on the LIM and SH3 domain protein 1 (LASP1): a versatile structural, signaling, and biomarker protein. *Oncotarget* **6**, 26–42
39. Zhao, T., Ren, H., Li, J., Chen, J., Zhang, H., Xin, W., Sun, Y., Sun, L., Yang, Y., Sun, J., Wang, X., Gao, S., Huang, C., Zhang, H., Yang, S., and Hao, J. (2015) LASP1 is a HIF1 α target gene critical for metastasis of pancreatic cancer. *Cancer Res.* **75**, 111–119
40. Traenka, C., Remke, M., Korshunov, A., Bender, S., Hielscher, T., Northcott, P. A., Witt, H., Ryzhova, M., Felsberg, J., Benner, A., Riester, S., Scheurlen, W., Grunewald, T. G., von Deimling, A., Kulozik, A. E., et al. (2010) Role of LIM and SH3 protein 1 (LASP1) in the metastatic dissemination of medulloblastoma. *Cancer Res.* **70**, 8003–8014
41. Keicher, C., Gambaryan, S., Schulze, E., Marcus, K., Meyer, H. E., and Butt, E. (2004) Phosphorylation of mouse LASP-1 on threonine 156 by cAMP- and cGMP-dependent protein kinase. *Biochem. Biophys. Res. Commun.* **324**, 308–316
42. Butt, E., Gambaryan, S., Göttfert, N., Galler, A., Marcus, K., and Meyer, H. E. (2003) Actin binding of human LIM and SH3 protein is regulated by cGMP- and cAMP-dependent protein kinase phosphorylation on serine 146. *J. Biol. Chem.* **278**, 15601–15607
43. Grunewald, T. G., Kammerer, U., Schulze, E., Schindler, D., Honig, A., Zimmer, M., and Butt, E. (2006) Silencing of LASP-1 influences zyxin localization, inhibits proliferation and reduces migration in breast cancer cells. *Exp. Cell Res.* **312**, 974–982
44. Grunewald, T. G., Kammerer, U., Winkler, C., Schindler, D., Sickmann, A., Honig, A., and Butt, E. (2007) Overexpression of LASP-1 mediates migration and proliferation of human ovarian cancer cells and influences zyxin localisation. *Br. J. Cancer* **96**, 296–305
45. Hailer, A., Grunewald, T. G., Orth, M., Reiss, C., Kneitz, B., Spahn, M., and Butt, E. (2014) Loss of tumor suppressor mir-203 mediates overexpression of LIM and SH3 protein 1 (LASP1) in high-risk prostate cancer thereby increasing cell proliferation and migration. *Oncotarget* **5**, 4144–4153
46. Zhao, L., Wang, H., Liu, C., Liu, Y., Wang, X., Wang, S., Sun, X., Li, J., Deng, Y., Jiang, Y., and Ding, Y. (2010) Promotion of colorectal cancer growth and metastasis by the LIM and SH3 domain protein 1. *Gut* **59**, 1226–1235
47. Tang, R., Kong, F., Hu, L., You, H., Zhang, P., Du, W., and Zheng, K. (2012) Role of hepatitis B virus X protein in regulating LIM and SH3 protein 1 (LASP-1) expression to mediate proliferation and migration of hepatoma cells. *Virol. J.* **9**, 163
48. He, B., Yin, B., Wang, B., Chen, C., Xia, Z., Tang, J., Yuan, Y., Feng, X., and Yin, N. (2013) Overexpression of LASP1 is associated with proliferation, migration and invasion in esophageal squamous cell carcinoma. *Oncol. Rep.* **29**, 1115–1123
49. Díaz, J. F., and Andreu, J. M. (1993) Assembly of purified GDP-tubulin into microtubules induced by taxol and taxotere: reversibility, ligand stoichiometry, and competition. *Biochemistry* **32**, 2747–2755
50. El-Deiry, W. S. (2003) The role of p53 in chemosensitivity and radiosensitivity. *Oncogene* **22**, 7486–7495
51. Zhou, J., and Wang, W. (2011) Analysis of microRNA expression profiling identifies microRNA-503 regulates metastatic function in hepatocellular cancer cell. *J. Surg. Oncol.* **104**, 278–283
52. Castro, D. S., Skowronska-Krawczyk, D., Armant, O., Donaldson, I. J., Parras, C., Hunt, C., Critchley, J. A., Nguyen, L., Gossler, A., Göttgens, B., Matter, J. M., and Guillemot, F. (2006) Proneural bHLH and Brn proteins coregulate a neurogenic program through cooperative binding to a conserved DNA motif. *Dev. Cell* **11**, 831–844
53. Jiang, L., Deng, J., Zhu, X., Zheng, J., You, Y., Li, N., Wu, H., Lu, J., and Zhou, Y. (2012) CD44 rs13347 C>T polymorphism predicts breast cancer risk and prognosis in Chinese populations. *Breast Cancer Res.* **14**, R105